Propagation Characteristics of Wideband Relay Channels in Urban Environment

Jianhua Zhang, Di Dong, Xin Nie,
Yangping Liang, Chengxiang Huang
Beijing University of Posts and Telecommunications
Email: jhzhang@bupt.edu.cn

Guangyi Liu, Weihui Dong
Research Institute of China Mobile
Email: liuguangyi@chinamobile.com

***Abstract*—In order to evaluate the relay performance for IMT-Advanced systems, the propagation characteristics of relay channels are necessary, especially in urban environments. We conducted wideband relay channel measurements at 2.35GHz in urban environments of China by employing a real-time channel sounder. Three types of links, i.e. base station to mobile station (BS-MS), relay station to mobile station (RS-MS) and base station to relay station (BS-RS), were measured separately at three sites. Statistical propagation characteristics are presented and compared in this paper, including path loss (PL), root mean square (rms) delay spread (DS), angular spread (AS) and cross-polarization discrimination (XPD). These results are necessary for the technical research and evaluation of the relay system.**

I. Introduction

Recently, the relay system has attracted lots of attention as it has several advantages over conventional cellular system, such as coverage extension, capacity improvement, reduction in power consumption and cooperative diversity [1]–[3]. It is considered as one of the possible techniques for IMT-Advanced and LTE+ systems. However, the actual performance of relay system highly depends on the channel conditions, such as large scale fading and small scale fading distribution, including delay spread (DS) and angular spread (AS). The large scale fading effects are important for coverage prediction and interference analysis of the relay system and the delay characteristic reveals the frequency selectivity of the wideband channel. Moreover, AS of each cluster and composite AS affect both ergodic and outage capacity and cross-polarization discrimination (XPD) determines the polarization diversity gain. Thus the properties of relay channel should be exactly modeled to validate its performance. At the same time, the model must be simple and sufficiently accurate for the sake of simulation.

Most of existing work on relay-based systems has been carried out under simplified assumptions for the channel properties [4]–[6]. The small scale fading is often assumed as Rayleigh distributed, regardless of whether the propagation condition is line of sight (LOS) or non-LOS (NLOS). The path loss (PL) of three separate links are supposed to follow the same propagation model. The propagation characteristics of relay channel are influenced by the geographic conditions and the antenna height of RS, BS and MS. It raises a question whether the current model can be applied to the link from RS to MS, since the antenna height at RS may be very low under most circumstances [7]. Channel measurement is the most straightforward approach to obtain propagation characteristics. However, the difficulty to measure and model relay channel is that there exists two more links, i.e. RS-MS and BS-RS (Fig. 1). A few relay channel measurements have been reported in [8], [9], which mainly concentrated on the relay performance in indoor environments. An outdoor relay channel measurement is presented in [10], but little attention is paid to propagation characteristics. Although the relationship between antenna height and channel characteristics has been investigated in [11] and [12], they were not dedicated to frequency bands allocated to the IMT-advanced system, which will probably utilize relay techniques.

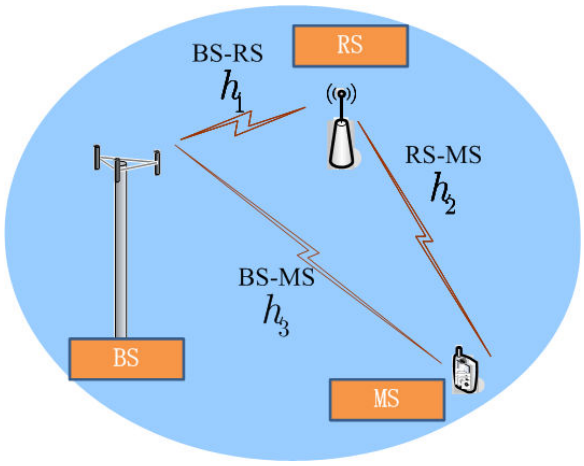

Fig. 1. Illustration of the relay system.

In order to investigate the characteristics of outdoor relay channels, we conducted a measurement campaign at the center frequency of 2.35GHz with a chip rate of 100 MHz utilizing the sounder from Elektrobit [13]. In this paper, PL is modeled in the log-distance expression based on measured channel impulse responses (CIRs). The empirical cumulative distribution functions (CDFs) of the rms DS is statistically summarized. Moreover, the Spatial-Alternating Generalized Expectation - maximization (SAGE) [14] algorithm is utilized to extract the double-directional spatial parameters from measured CIRs. Then AS at BS, RS and MS are presented based on the estimated results from SAGE. Due to the antenna height of

RS, the channels of BS-RS and RS-MS link manifest different characteristic from conventional link BS-MS.

The rest of the paper is organized as follows. In Section II, the measurement system and environments are described. In Section III presents the estimation approach of channel parameters. In Section IV, the channel characteristics are presented from three perspectives, i.e. PL, DS and AS. Finally, some conclusions are drawn in Section V.

II. Measurements Description

A. Measurement System

Measurements were performed in downtown Beijing. A pseudo-random sequence of length 1023 was continuously generated at the transmitter (TX) with a chip rate of 100 MHz. At the receiver (RX), CIRs were obtained by slide correlating the received signal with a synchronized copy of the sequence. The channel sampling frequency was 120.98 Hz. Different antenna configurations were applied for different measurement purpose: a single vertical-polarized dipole was employed at BS, RS and MS, respectively, in order to capture the large scale and delay domain parameters; instead, to obtain the spatial domain parameters, omni-directional array (ODA) consisting of 16 antenna elements was utilized. The transmit power at antenna input was 26 dBm.

B. Measurement Environment

The measurement environment can be characterized as typical urban with the average building height of 20 m and building density of about 30%. Three measurement sites were involved, which are denoted as S1, S2 and S3. Fig. 2(a) and 2(b) show the air views of the measurement environment. In S1, the BS (BS1) antenna was mounted on the rooftop of a building which was about 20m in height. The RS (RS1) antenna was located on the north side of the gymnasium. The BS (BS2) antenna in S2 was on the same rooftop just a few meters away from BS1 and the RS (RS2) antenna was installed on the west stand of the playground. As for S3, the BS (BS3) antenna is deployed on the top of a 5-floor high building, which is about 22m in height. The RS antenna was fixed on the top of a testing vehicle. Considering the height of the relay antenna does not need to be as high as the BS in order to reduce operating and maintenance costs [2], the antenna height of RS1, RS2 and RS3 were set to 6.8m, 7.0m and 7.0m, respectively. The MS antenna was fixed on a trolley, moving at a velocity of about 0.5 m/s along the routes shown in Fig. 2(a) and 2(b).MS positions were recorded using the GPS. As the relay is expected to cover a smaller region compared to the BS [1], the maximum distance between TX and RX in the measurement was about 250 m. The detailed measurement information is listed in Table I.

III. Channel Parameter Estimation

After the measurement, post-processing was implemented to estimate the channel parameters. In order to seperate the noise from the measured multipath components (MPCs), the dynamic range is set as 20dB from the strongest path for both

(a) Site 1 and 2.

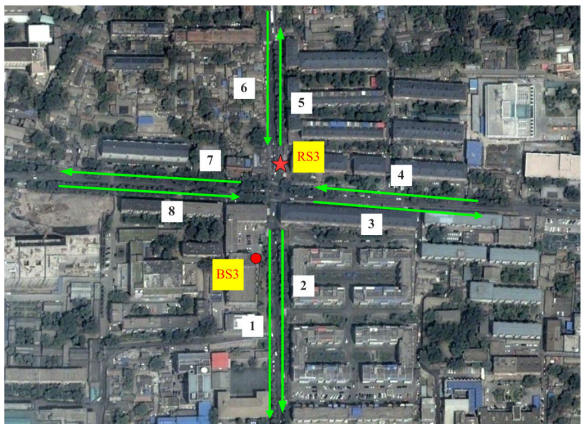

(b) Site 3.

Fig. 2. Measurement environment and route plans at three sites.

TABLE I
Detailed Measurement Information

Items	S1	S2	S3
BS antenna height	20 m	20 m	22 m
RS antenna height	6.8 m	7.0 m	7.0 m
MS antenna height	1.8 m	1.8 m	1.8 m
BS-RS distance	144 m	58 m	106 m
BS-RS propagation condition	NLOS	LOS	LOS
MS velocity	0.5 m/s	0.5 m/s	0.5 m/s
Measurement mode	downlink	downlink	downlink
Number of antennas (BS, RS, MS)	1,1,1	1,1,1	16,16,16

LOS and NLOS cases. In this section, the estimation procedure of path loss, shadow fading, rms delay/angular spread and cross polarization ratio is presented.

A. Path Loss and Shadow Fading

As path loss and shadow fading are large scale parameters, they are extracted from a set of small areas called *local area* (LA), where only small scale fading takes place. Define the vector $\boldsymbol{r} = (x, y)$ as the location of MS at any instance with

the coordinates of RS as $(0,0)$. We use the expression in [15], letting $\mathcal{A}(\boldsymbol{r};R)=\{\boldsymbol{s}_1,\boldsymbol{s}_2,\cdots,\boldsymbol{s}_N\}$ be the set of measurement positions within the LA centered at $\boldsymbol{r}$ of radius R, where N is the cardinality of $\mathcal{A}(\boldsymbol{r};R)$. The joint effect of path loss, shadow fading and antenna gain is written as

$$E(\boldsymbol{r})=\frac{1}{N}\sum_{n=1}^{N}\int|h(\tau;\boldsymbol{s}_n)|^2\mathrm{d}\tau,\quad \boldsymbol{s}_n\in\mathcal{A}(\boldsymbol{r};R). \tag{1}$$

where $h(\tau;\boldsymbol{s}_n)$ is the nth channel impulse response within the local area. Denoting the path loss, shadow fading and antenna gain as $L(\boldsymbol{r})$, $S(\boldsymbol{r})$ and G_{A}, respectively, all in decibels. $E(\boldsymbol{r})$ in decibels is given by

$$E_{\mathrm{dB}}(\boldsymbol{r})=G_{\mathrm{A}}-L(\boldsymbol{r})-S(\boldsymbol{r}). \tag{2}$$

The single-slope and double-slope log-distance model are adopted to estimate the path loss for LOS and NLOS cases, respectively. The two models are given as

$$L(\boldsymbol{r})=a_1+10n_1\cdot\log_{10}\|\boldsymbol{r}\|, \tag{3}$$

$$L(\boldsymbol{r})=\begin{cases}a_2+10n_2\cdot\log_{10}\|\boldsymbol{r}\| & \|\boldsymbol{r}\|\leqslant d_{\mathrm{BP}},\\ a_3+10n_3\cdot\log_{10}\big(\|\boldsymbol{r}\|/d_{\mathrm{BP}}\big) & \|\boldsymbol{r}\|>d_{\mathrm{BP}},\end{cases} \tag{4}$$

where n_i and $a_i(i=1,2,3)$ are the path loss exponent and intercept, respectively. $\|\boldsymbol{r}\|$ represents the TX-RX distance in meters and d_{BP} is the break point distance. Linear regression in a minimum mean square error (MMSE) sense is utilized to estimate a_i and n_i. Finally, shadow fading at position $\boldsymbol{r}$ can be obtained from (2).

B. Delay Spread

The rms DS is crucial in system design. It is determined by the power delay profile at local area. It is calculated as the standard deviation of the excess delay weighted with the power which is given by

$$\tau_{\mathrm{rms}}=\sqrt{\left(\sum_{l=1}^{L}P_l\right)^{-1}\sum_{l=1}^{L}P_l\tau_l^2-\left(\sum_{l=1}^{L}P_l\right)^{-2}\left(\sum_{l=1}^{L}P_l\tau_l\right)^2} \tag{5}$$

where τ_l and P_l denote respectively, the excess delay and power of the lth path.

C. Angular Spread

In order to extract the spatial characteristics from the measured CIRs, the SAGE algorithm is utilized to estimate the parameters of MPCs.

Angle spread is an important parameter which evaluates the dispersion in angular domain. The angle spread is calculated as the root second central moment of power angular spectrum. To avoid the ambiguous effect due to the circular wrapping of the angles, the circular AS (CAS) is calculated. This AS is constant regardless of the value of the angle shift, as in the case described in the 3GPP spatial channel model (SCM) specifications. The CAS is defined as

$$\sigma_{AS}=\arg\min_{\Delta}\sigma_{AS}(\Delta)=\sqrt{\sum_{l=1}^{L}\theta_{l,\mu}(\Delta)^2P_l\cdot\left(\sum_{l=1}^{L}P_l\right)^{-1}}, \tag{6}$$

where P_l is the power of the lth path. $\theta_{l,\mu}(\Delta)$ is given by

$$\theta_{l,\mu}(\Delta)=\begin{cases}2\pi+\omega & \omega<-\pi,\\ \omega & -\pi\leqslant\omega\leqslant\pi,\\ 2\pi-\omega & \omega>\pi,\end{cases} \tag{7}$$

where ω can be written as

$$\omega=\theta_l(\Delta)-\sqrt{\sum_{l=1}^{L}\theta_l(\Delta)P_l\cdot\left(\sum_{l=1}^{L}P_l\right)^{-1}}, \tag{8}$$

$$\theta_l(\Delta)=\theta_l+\Delta. \tag{9}$$

in which θ_l is the angle of the lth path estimated by SAGE and Δ denotes the angle shift ranging from $-\pi$ to π.

D. Cross-Polarizarion Discrimination

Cross-Polarization Discrimination has an important influence on the diversity gain. XPD is defined as the co-polarized received signal power to the cross-polarized received power, which is given by

$$\mathrm{XPD}_V=10\cdot\log_{10}\left(\left|\frac{\alpha_{V,V}}{\alpha_{H,V}}\right|^2\right)(\mathrm{dB}), \tag{10}$$

$$\mathrm{XPD}_H=10\cdot\log_{10}\left(\left|\frac{\alpha_{H,H}}{\alpha_{V,H}}\right|^2\right)(\mathrm{dB}). \tag{11}$$

The entry $\alpha_{p,q},p\in\{V,H\},q\in\{V,H\}$ is the complex gain of q-to-p polarization of the MPC and they are estimated using the SAGE algorithm.

IV. Measurement Results and Discussion

A. Path Loss and Shadow Fading

The measured power loss of the RS-MS link and the estimated path loss are shown in Fig. 3(a) and 3(b) for both LOS and NLOS cases, respectively. In the case of LOS, the results from S1 and S2 are plotted together, for the similar break point distance. It is observed that the double-slope model can well fit the measured power loss, and the estimated n_2 is 2.07, which is quite close to that of free space model. Beyond the break point distance, path loss exponent rises up to 3.75. Since the antenna height of RS is below the average building height, urban microcell (UMi) path loss model recommended by ITU-R [16] and the IEEE 802.16j Type-F path loss model [7] are selected for comparison. It is noticed that the UMi LOS model is below the free space model before the break point distance and is also about 3 dB below the estimated path loss. It indicates that the UMi LOS model may underestimate the power loss within a short distance range when applied to the RS-MS link. Comparatively, the 802.16j model provides a better prediction.

As for the NLOS case, the number of power loss samples is fewer due to the power constraint at TX. The NLOS path loss model for IEEE 802.16j Type-F scenario is geometry-based, which is difficult to be compared with our results when the MS was obstructed by irregular-shaped objects like trees and cars. Therefore, only UMi path loss model is chosen.

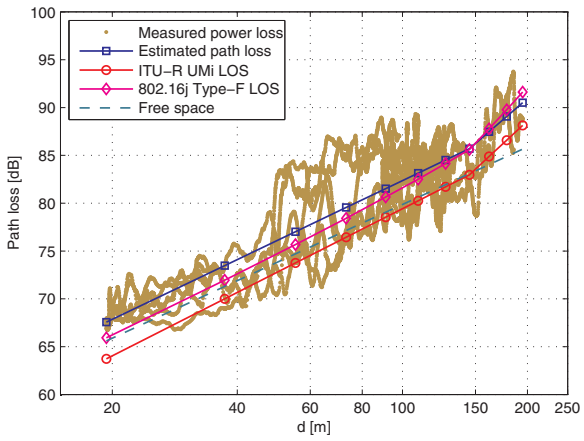

(a) The LOS case.

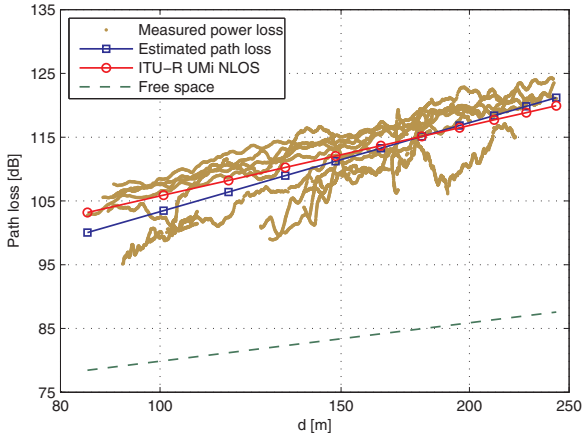

(b) The NLOS case.

Fig. 3. Path loss of the RS-MS link for (a) LOS and (b) NLOS cases.

TABLE II
THE ESTIMATED PATH LOSS PARAMETERS FOR BOTH LOS AND NLOS CASES

Cases	n_1	n_2	n_3	a_1	a_2	a_3
	[dB/ $\log_{10}$ m]			[dB]		
LOS	2.07	3.75	-	40.9	85.7	-
NLOS	-	-	4.64	-	-	10.6

Although the lower antenna height may lead to higher path loss, our result shows that the estimated path loss is below the UMi NLOS model when the TX-RX distance is less than 177 m. However, the estimated path loss exponent is 4.64, which makes the path loss exceed the UMi NLOS model when the distance reaches 177 m and further. This is owing to the fact that the main obstructing objects located at a short distance in the measurement environment were trees and traffics, which caused less power attenuation, while the buildings were located at the edge of the coverage area. In general, the estimated path loss and the UMi NLOS model are fairly close within the measurement range. The estimated path loss parameters are summarized in Table II.

The shadow fading in decibels can be well modeled as a zero mean Gaussian RV. The standard deviation (std.) of the overall shadow fading is 3.1 dB.

TABLE III
THE EMPIRICAL STATISTICS OF RMS DS FOR VARIOUS LINKS

Link		μ_τ [lg(s)]	σ_τ [lg(s)]	$\overline{\tau}$ [ns]
LOS	BS-MS	-7.03	0.26	96
	RS-MS	-7.05	0.26	95
NLOS	BS-MS	-6.44	0.08	373
	RS-MS	-6.83	0.18	158
BS-RS		–	–	15

B. Delay Spread

Early literatures have justified that the rms DS turns out a random variable related to the Tx-Rx distance [17]. Log-normal distribution is traditionally applied to describe the behavior of random rms DS. Since in links involved RS, the following aspects should be taken into account:

a) **scatters**. Compared to that of BS, the decrease of antenna height leads to more dense scattering surrounding the RS;

b) **Tx-Rx distance**. Introduction of relay station reduces the propagation distance in either BS-RS or RS-MS link;

c) **mobility**. As for the link between BS and fixed RS, the scatters surrounding both ends and Tx-Rx distance rarely vary. Therefore, the randomization of rms DS might be diminished in a certain degree.

The empirical statistics of rms DS are listed in Table III, where various links involved relay station are compared. The μ_τ and σ_τ denote the fitting results of mean value and std., respectively, when log-normal distribution is applied to fitting. And $\overline{\tau}$ is the mean value calculated from all samples of RDS. The relation between them is determined by

$$\lg \overline{\tau} = \mu_\tau + \frac{\sigma_\tau^2 \cdot \ln 10}{2} . \tag{12}$$

In LOS case, the behaviors of rms DS for BS-MS and RS-MS links are similar, since approximate statistical parameters are observed. Due to the existence of dominant component, the impacts of variation in dispersion paths are not evident. Whereas in NLOS environment, the mean value of $\overline{\tau}$ decreases from 373 ns of BS-MS link to 158 ns in RS-MS case. The result indicates that introducing RS achieves considerable reduction of delay spread. The main reason involves the decrease of Tx-Rx distance.

In BS-RS link, however, the log-normal distribution can no longer fit the randomization of rms DS. Actually, the rms DS exists at 15 ns with a probability up to 68% in the fixed-fixed link. We thus propose to treat it as an invariable parameter in channel modeling.

C. Angular Spread

Table IV depicts the statistics of the CAS of RS-MS link obtained from the measurement at S3. In the table, μ_A and σ_A are the parameters of the log-normal distributions when they are fitted to the CAS observations. The results demonstrate that

TABLE IV
STATISTICAL COMPARISON BETWEEN THE MEASURED CAS OF RS-MS LINK AND ITU STANDARD.

link		RS-MS		ITU-R [16]	
propagation condition		LOS	NLOS	LOS	NLOS
CAS of AoD	μ_A[lg(deg)]	1.25	1.48	1.20	1.41
	σ_A[lg(deg)]	0.29	0.16	0.43	0.17
	mean[deg]	21.6	31.9	15.8	25.7
CAS of AoA	μ_A[lg(deg)]	1.40	1.56	1.75	1.84
	σ_A[lg(deg)]	0.24	0.18	0.19	0.15
	mean[deg]	28.5	38.9	56.2	69.2

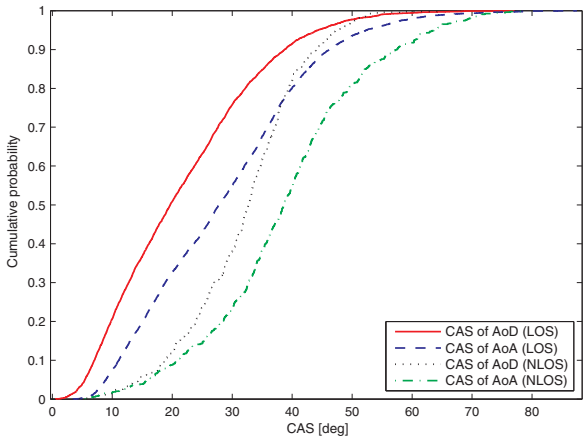

Fig. 4. The CDFs of CAS for LOS and NLOS cases.

at the same side, the CAS in the NLOS case is larger than that in the LOS case. It indicates the fact that in the NLOS case, MPCs go through more scatterings and reflections. The results also represent that the CAS of AoA is lager than that of AoD for both LOS and NLOS scenario. It is reasonable as there are richer local scatterers along the mobile route for the MS than that surrounding the fixed RS. By contrast to the UMi scenario described in ITU-R M.2135 [16], the CAS of AoD is larger in both LOS and NLOS case. One reason resulting in this effect could be the fact that the antenna height of RS is lower than that of BS in urban micro cell. As a consequence, the MPCs interact with more scatterers within the local area when transmitted from RS, which lead to lager CAS. On the contrary, the observed CAS of AoA is smaller than that in the UMi scenario described in ITU-R M.2135. It could be due to the fact that in the considered environment, the MS moves in the street canyon, thus the streets perform a wave-guided effect, which makes most of the MPCs impinge at the MS within a small range in the angular domain. The cumulative distribution functions (CDF) of CASs are shown in Fig. 4.

D. Cross-Polarization Discrimination

There is a general consensus in the literature that the XPD, when expressed in dB, has a non-zero-mean Gaussian distribution [18]. Hence we can model the distribution of the XPD as XPD $\sim \mathcal{N}(\mu, \sigma^2)$. The mean value μ and standard deviation σ of the XPD are obtained by utilizing least square fitting. The μ and σ of XPD_V for BS-RS link are 7.98 dB and 8.00 dB, meanwhile, the μ and σ of XPD_H for BS-RS link are 5.98 dB and 8.98 dB. The Gaussian fitting results for BS-MS and RS-MS links are given in Table V.

TABLE V
GAUSSIAN FITTING RESULTS FOR BS-MS LINK AND RS-MS LINK

	BS-MS		RS-MS	
	μ	σ	μ	σ
XPD_V LOS	4.37	8.07	2.86	8.38
XPD_H LOS	5.06	8.54	2.19	8.35
XPD_V NLOS	6.84	8.43	7.62	7.93
XPD_H NLOS	2.45	8.25	1.23	8.33

The XPD values for BS-RS link are high indicating little cross-coupling between the orthogonal states of polarization. It can be found from Table V that except XPD_V in NLOS scenario, the XPDs of BS-MS link are larger than those of RS-MS link. The main reason is that due to the lower RS antennas, the increased scatters result in a greater degree of depolarization. We also observe that the XPD_V and XPD_H are almost the same in LOS scenario. However, in NLOS scenario, there is a big difference between XPD_V and XPD_H. For the RS-MS link, the difference becomes more remarkable. The result indicate that the vertical polarization preserves better than the horizontal polarization during the propagation, especially in the RS-MS link where the RS antennas are relatively lower.

V. CONCLUSION

This paper presents characteristics of relay channels in the urban scenario of China. Based on the extensive channel measurements, parameters of the empirical log-distance PL models are obtained. Measurement results showed that the current IMT-Advanced channel model may under estimate the path loss at a short TX-RX distance for the LOS case. The estimated path loss exponent for the NLOS case was also larger than that in the current model. Moreover, in LOS case, the behaviors of rms DS for BS-MS and RS-MS links are similar and in NLOS case, the mean value of rms DS decreases from 373 ns of BS-MS link to 158 ns in RS-MS case. Compared to current IMT-Advanced channel model, the CAS of AoD is larger in both LOS and NLOS case. On the contrary, the observed CAS of AoA is smaller than that of IMT-Advanced channel model.The XPD values for BS-RS link are high indicating little cross-coupling between the orthogonal states of polarization and the diversity gain could be achieved easily.

ACKNOWLEDGMENT

The research was supported in part by National 863 High Technology Research and Development Program of China under Grant No. 2006AA01Z258, and by the Research Institute of China Mobile.

The authors would like to thank all members from BUPT and Elektrobit Corporation, Finland for their great efforts

in the measurement campaigns. Especially thanks to China Mobile Research Institute to coordinate the measurement sites.

REFERENCES

[1] A. Nosratinia, T. E. Hunter, and A. Hedayat, "Cooperative communication in wireless networks," *IEEE Commun. Mag.*, vol. 42, no. 10, pp. 74–80, Oct. 2004.

[2] R. Pabst, B. H. Walke, D. C. Schultz, P. Herhold *et al.*, "Relay-based deployment concepts for wireless and mobile broadband radio," *IEEE Commun. Mag.*, vol. 42, no. 9, pp. 80–89, Sept. 2004.

[3] L. Jianing, Z. Jianhua, Y. Zhang, and P. Zhang;, "A comparison of tdma, dirty paper coding and beamforming for multiuser mimo relay networks," *Journal on Communications and Networks, Special Issue on Cooperative Communication and Its Applications*, June 2008.

[4] J. Laneman, G. Wornell, and D. Tse, "An efficient protocol for realizing cooperative diversity in wireless networks," in *Proc. IEEE ISIT*, 2001, p. 294.

[5] R. Nabar, H. Bolcskei, and F. Kneubuhler, "Fading relay channels: Performance limits and space-time signal design," *IEEE J. Sel. Areas Commun.*, vol. 22, no. 6, pp. 1099–1109, 2004.

[6] B. Wang, J. Zhang, and A. Host-Madsen, "On the capacity of MIMO relay channels," *IEEE Trans. Inf. Theory*, vol. 51, no. 1, pp. 29–43, 2005.

[7] IEEE 802.16j-06/013r3, "Multi-hop relay system evaluation methodology (channel model and performance metric)," Feb. 2007. [Online]. Available: http://wirelessman.org/relay/docs/80216j-06_013r3.pdf

[8] P. Kyritsi, P. Eggers, R. Gall, and J. Lourenco, "Measurement based investigation of cooperative relaying," in *Proc. IEEE VTC*, Fall 2006, pp. 1–5.

[9] Y. Haneda, V. Kolmonen, and T. Riihonen, "Evaluation of relay transmission in outdoor-to-indoor propagation channels." [Online]. Available: http://www.cost2100.org/uploads/File/Workshop/Proceedings/W08114.pdf.

[10] L. Jiang, L. Thiele, and V. Jungnickel, "Modeling and measurement of MIMO relay channels," in *Proc. IEEE VTC*, Spring 2008, pp. 419–423.

[11] M. Feuerstein, K. Blackard, T. Rappaport, S. Seidel *et al.*, "Path loss, delay spread, and outage models as functions of antenna height for microcellular system design," *IEEE Trans. Veh. Technol.*, vol. 43, no. 3, pp. 487–498, 1994.

[12] E. Benner and A. Sesay, "Effects of antenna height, antenna gain, and pattern downtilting for cellular mobile radio," *IEEE Trans. Veh. Technol.*, vol. 45, no. 2, pp. 217–224, 1996.

[13] Elektrobit, "Propsound CS: The ultimate technology in radio propagation measurement." [Online]. Available: http://www.propsim.com/file.php?732

[14] B. H. Fleury, M. Tschudin, R. Heddergott, D. Dahlhaus *et al.*, "Channel parameter estimation in mobile radio environments using the sage algorithm," *IEEE J. Sel. Areas Commun.*, vol. 17, no. 3, pp. 434–450, March 1999.

[15] Y. Zhang, J. Zhang, D. Dong, X. Nie *et al.*, "A novel spatial autocorrelation model of shadow fading in urban macro environments," in *Proc. IEEE GLOBECOM*, 2008, pp. 1–5.

[16] "Rep. ITU-R M.2135 Guidelines for evaluation of radio interface technologies for IMT-Advanced," Oct. 2008.

[17] L. J. Greenstein, V. Erceg, Y. S. Yeh, and M. V. Clark, "A new path-gain/delay-spread propagation model for digital cellular channels," *IEEE Trans. Veh. Technol.*, vol. 46, no. 2, pp. 477–485, May 1997.

[18] M. Shafi, M. Zhang, A. Moustakas, P. Smith *et al.*, "Polarized mimo channels in 3d: models, measurements and mutual information," *IEEE J. Sel. Areas Commun.*, vol. 24, no. 3, pp. 514–527, 2006.